JPP Journal of Pharmacy and Pharmacology
ROYAL PHARMACEUTICAL SOCIETY

# Preparation and characterisation of novel spray dried nano-structured para-aminosalicylic acid particulates for pulmonary delivery: impact of ammonium carbonate on morphology, chemical composition and solid state



| | |
|---|---|
| Journal: | *Journal of Pharmacy and Pharmacology* |
| Manuscript ID: | JPP-11-0759.R1 |
| Wiley - Manuscript type: | Research Paper |
| Date Submitted by the Author: | n/a |
| Complete List of Authors: | Gad, Shadeed; University of Dublin, Trinity College Dublin, School of Pharmacy and Pharmaceutical Sciences<br>Tajber, Lidia; University of Dublin, Trinity College Dublin, School of Pharmacy and Pharmaceutical Sciences<br>Corrigan, Owen; University of Dublin, Trinity College Dublin, School of Pharmacy and Pharmaceutical Sciences<br>Healy, Anne Marie; University of Dublin, Trinity College Dublin, School of Pharmacy and Pharmaceutical Sciences |
| Keywords: | Dosage Form Design and Characterisation < Pharmaceutics and Drug Delivery, Drug Delivery to Specific Tissues < Pharmaceutics and Drug Delivery |
| Abstract: | Objectives: The objective of this work was to spray dry p-aminosalicylic acid (PAS) and its ammonium salt and to investigate the impact of the pore forming agent, ammonium carbonate (AC), on the morphological, aerodynamic and physicochemical properties of the resulting powders.<br>Methods: Microparticles were prepared by spray drying from ethanol/water solvent systems. Their solid state properties were evaluated by SEM, pXRD, DSC, TGA and in vitro deposition, using the twin impinger.<br>Key findings: The physicochemical properties of PAS were altered on spray drying with AC and a new solid state was produced. The solution composition impacted on the morphology of the resulting powders, which ranged from irregular crystal agglomerates to spherical crystal clusters and porous microparticles. The chemical composition, structure and morphology were dependent on process inlet temperature, low inlet temperatures resulting in a novel solid of stoichiometry; PAS:ammonia:water, 2:1:0.5. At higher temperatures pure PAS was obtained. In vitro deposition studies showed an |

| | |
|---|---|
| | increase in emitted dose from spray dried drug, relative to the micronised PAS.<br>Conclusions: Under appropriate process conditions AC interacts with the acidic PAS, resulting in the formation of a novel solid state drug phase. Spray dried PAS powders have potential for pulmonary delivery. |
| | |

# Preparation and characterisation of novel spray dried nano-structured para-aminosalicylic acid particulates for pulmonary delivery: impact of ammonium carbonate on morphology, chemical composition and solid state

Shadeed Gad, Lidia Tajber, Owen I. Corrigan and Anne Marie Healy*

School of Pharmacy and Pharmaceutical Sciences, University of Dublin, Trinity College Dublin, Dublin 2, Ireland

* To whom correspondence should be sent.

Dr. Shadeed Gad – e-mail: gads@tcd.ie, Ph.: 00 353 1896 2809, Fax.: 00 353 1896 2783

Dr. Lidia Tajber – e-mail: lidia.tajber@tcd.ie, Ph.: 00 353 1896 2787, Fax.: 00 353 1896 2783

Prof. Owen I. Corrigan – e-mail: ocorrign@tcd.ie, Ph.: 00 353 1896 2782, Fax.: 00 353 1896 2783

Dr. Anne Marie Healy – e-mail: healyam@tcd.ie, Ph.: 00 353 1896 1444, Fax.: 00 353 1896 2783

Keywords: p-aminosalicylic acid, spray drying, new solid-state form, aerosol, inhalation

## Abstract

Objectives: The objective of this work was to spray dry p-aminosalicylic acid (PAS) and its ammonium salt and to investigate the impact of the pore forming agent, ammonium carbonate (AC), on the morphological, aerodynamic and physicochemical properties of the resulting powders.

Methods: Microparticles were prepared by spray drying from ethanol/water solvent systems. Their solid state properties were evaluated by SEM, pXRD, DSC, TGA and *in vitro* deposition, using the twin impinger.

Key findings: The physicochemical properties of PAS were altered on spray drying with AC and a new solid state was produced. The solution composition impacted on the morphology of the resulting powders, which ranged from irregular crystal agglomerates to spherical crystal clusters and porous microparticles. The chemical composition, structure and morphology were dependent on process inlet temperature, low inlet temperatures resulting in a novel solid of stoichiometry; PAS:ammonia:water, 2:1:0.5. At higher temperatures pure PAS was obtained. *In vitro* deposition studies showed an increase in emitted dose from spray dried drug, relative to the micronised PAS.

Conclusions: Under appropriate process conditions AC interacts with the acidic PAS, resulting in the formation of a novel solid state drug phase. Spray dried PAS powders have potential for pulmonary delivery.

## 1. Introduction

Inhaled therapy is potentially a convenient way of delivering antitubercular agents to the lungs. Tuberculosis continues to be an important killer disease causing three million deaths annually [1]. It is a chronic infectious disease caused by the bacterium *Mycobacterium tuberculosis*, and the lungs are the primary site of infection. Although potentially curative treatments and vaccines are available, tuberculosis remains the foremost cause of preventable deaths in the world. Difficulties associated with the treatment of tuberculosis include low concentrations of the drugs in the lungs following oral administration and high lung clearance [2] as well as long treatment times, up to two years, where poor compliance can result in the development of multidrug-resistant strains of *M. tuberculosis* [3].

p-Aminosalicylic acid (PAS, Figure 1a) is used therapeutically as an antitubercular agent and needs to be administered orally in very large amounts, 8 - 12 grams per day in 2 or 3 divided doses [4]. This is inconvenient to the patient, hence the importance of reducing the drug dosage. Formulation of PAS into porous particles for direct delivery into the lungs was described by Tsapis et al. [5]. They formulated PAS as large porous particles containing 95% PAS by weight and the excipient 1,2-dipalmitoyl-sn-glycero-3-phosphocholine via spray drying. Pharmacokinetic data indicated that PAS delivered via insufflation reached the systemic circulation within 15 min of delivery to the lungs with a plasma peak concentration of 11±1 µg/ml. PAS was cleared within 3 h from the lung lining fluid and plasma but was still present at therapeutic concentrations in the lung tissue and the authors concluded that the total body dose was approximately 11 mg/kg via the lungs compared to an estimated value of 57 mg/kg for oral dosing of PAS in humans [5].

Recently, a novel spray drying technology was described, aimed at the production of nanoporous microparticles, NPMPs [6,7]. This method involves the use of co-solvents and process enhancers, for example ammonium carbonate, to produce particles suitable for dry powder inhalation drug delivery. It provides advantages over current technologies as it

involves a simple one-step particle engineering process and produces excipient-free microparticles suitable for inhalation, the volatile process enhancer being removed during the spray drying process [6].

As PAS is an acidic drug, the primary objective of this study was to explore the potential of ammonium carbonate, the process enhancer and an ionisable excipient, to interact with PAS during the spray drying process, thus producing a novel salt/complex form of the API. Of interest also was to ascertain if NPMPs of PAS could be produced and, subsequently, the processing parameters and spray drying conditions optimised to produce NPMPs with suitable micromeritic properties for inhalation. This is the first study by our group on the NPMP spray drying technology where we have employed an acidic drug. In the current study, the preparation and properties of spray dried PAS systems with and without the process enhancer, ammonium carbonate, were investigated. The particle size and morphology of all the powders produced were studied and subsequently some of these systems were selected for further characterisation by *in vitro* deposition using a twin impinger.

## 2. Materials and methods

### 2.1 Materials

p-Aminosalicylic acid (PAS), ammonium carbonate, ammonia assay kit were purchased from Sigma-Aldrich (Ireland). Potassium dihydrogen phosphate was obtained from Merck (Germany) and tetraoctylammonium bromide was purchased from Fluka (USA). Dimethylsulphoxide-D6 was obtained from Apollo Scientific (UK) ethanol (99.9% v/v, max. 20 ppm non-volatile content) was purchased from Cooley distillery (Ireland). HPLC grade methanol was purchased from Lab Scan Analytical Sciences (Ireland), and deionised water was produced by a Purite Prestige Analyst HP water purification system.

## 2.2 Preparation of ammonium salt of PAS

The ammonium salt of PAS (AM-PAS, Figure 1b) was prepared according to the method of Forbes et al. [8]. The preparation process involved the addition of 3.3 ml 35% ammonia solution with continuous stirring to a suspension of 10 g of the acid in 35 ml ethanol. The mixture was heated until a clear solution was obtained, which was then cooled for 2 hours with continuous stirring. The crystals were filtered and washed twice with 2 ml of ethanol. The recovered product was then dried in a desiccator under vacuum overnight.

## 2.3 Spray drying

PAS and AM-PAS systems were spray dried using a Büchi B-290 spray dryer (Büchi Laboratoriums-Technik AG, Switzerland) operating in the open mode configuration. Experimental conditions were: inlet air temperature 78 ℃, airflow rate of 670 Nl/h and aspirator rate 100%. Compressed air was used as the drying gas. Solutions for spray drying were prepared in aqueous-ethanolic solvents with or without ammonium carbonate as previously described by Healy et al. [6] and Nolan et al. [7]. Table 1 presents a summary of feed composition and process outlet temperatures.

## 2.4 Micronisation

Micronisation of PAS was performed using a Jet-O-Mizer fluid energy mill model 00. The drug compound was placed into the vibratory feeder. The vibratory feeder was set at 60% maximum vibrations. The vibratory feed rate is the rate at which the material to be micronised enters the Venturi feed and from there enters the grinding chamber where micronisation takes place. The grinding pressure and pusher pressure were set at 40 psi.

## 2.5 Solubility studies

PAS powder was added in an approximately 3-fold excess of estimated solubility to 10 ml of a solvent mixture contained in a glass, screw cap test tube. The following ethanol/water solvent systems were investigated: 90% ethanol/10% water v/v, 80% ethanol/20% water v/v

and 70% ethanol/30% water v/v. The tubes were shaken at 100 cpm in a thermostated water bath at 25 ℃ and analysed after 24 h when the equilibrium was reached. The suspensions were filtered through a 0.45 µm membrane filter and the filtrates were assayed by UV spectrophotometry (Pharmspec UV-1700, Shimadzu) at 280 nm.

**2.6 Thermal Analysis**

Differential Scanning Calorimetry (DSC) was performed on accurately weighed samples (2 – 6 mg) in closed 40 µl aluminium pans with three vent holes. Samples were run at a heating rate of 10ºC/minute under nitrogen purge from 25 – 300 ºC (except where otherwise indicated) using a Mettler Toledo DSC 821$^{e}$ (Mettler Toledo Ltd., Switzerland) [9]. Mettler Toledo STAR$^{e}$ software was used for analysis of thermal events.

Thermogravimetric analysis (TGA) was performed using a Mettler TG 50 (Mettler Toledo Ltd., Switzerland) linked to a Mettler MT 5 balance. Data was processed using Mettler Toledo STAR$^{e}$ software. Accurately weighed samples were analysed using open pans under nitrogen stream. Samples were run at a heating rate of 10ºC/minute from 25 – 300 ºC [9], except where otherwise indicated.

**2.7 Powder X-ray Diffraction (pXRD)**

pXRD scans were made on samples in low background silicon mounts, which consisted of cavities 0.5 mm deep and 9 mm in diameter (Bruker AXS, UK). A Siemens D500 diffractometer (Siemens AG, Germany) was used. This consists of a DACO MP wide range goniometer with a $1.0^{0}$ anti-scatter slit and a $0.15^{0}$ receiving slit. The Cu anode X-ray tube was operated at 40 kV and 30 mA in combination with a Ni filter to give monochromatic Cu Kα X-rays. Measurements were taken from 5º to 40º on the theta 2 scale at a step size of $0.05^{0}$ per second for qualitative analysis [9].

**2.8 Fourier Transform Infrared Spectroscopy (FTIR)**

FTIR was carried out using a Magna – IR 560 Spectrometer E.S.P. (Thermo Electron Corporation, U.S.A.) Fourier transform infrared spectrometer. Potassium bromide (KBr) discs were prepared based on 1 % sample loading. Discs were prepared by grinding the sample with KBr in an agate mortar and pestle, placing the sample in an evacuable KBr die and applying 8 tons of pressure, in an IR press [6]. The software used for processing the data was OMNIC E.S.P. (Thermo Electron Corporation, U.S.A.) software.

**2.9 Elemental analysis (CHN)**

The elemental analysis on PAS samples as presented in Table 2 was carried out using a CE440 CHN analyzer (Exeter Analytical, UK) as previously described [6].

**2.10 Nuclear magnetic resonance spectra (NMR)**

Nuclear magnetic resonance spectra of each sample were recorded on an Avance III 400 system (Bruker, Germany) at a proton frequency of 400.13 MHz and carbon frequency of 100.62 MHz. Dimethylsulphoxide-D6 was used as a solvent for PAS samples [10].

**2.11 Determination of degradation product of PAS in the presence of the drug**

A HPLC method was adopted to determine 3-aminophenol (the main degradation product of PAS in the presence of the drug [11]. Separation was carried out at ambient temperatures. The HPLC used was a Shimadzu LC-10AT VP liquid chromatograph with a Shimadzu L-10A system controller, a Shimadzu SPD-10A UV-VIS detector, a Shimadzu DGU-14 degasser and a SIL-10AD VP auto injector system. Samples were analysed using Shimadzu Class VP software (version 6.10). A Hypersil BDS C18 5µm, 150 mm × 4.6 mm column was used and a flow rate of 1.5 ml/min using a UV detector at 280 nm. The mobile phase was 55 parts methanol, 45 parts 0.05 M potassium phosphate buffer (pH 7.0) containing 1 mM tetraoctylammonium bromide as ion-pairing agent. The separation was carried out at ambient temperature. Limits of detection and quantitation were 0.1 and 0.5 µg/ml, respectively, while the precision was below 5% (RSD). The retention time of 3-aminophenol

(formed by decarboxylation of PAS, Figure 1c) was 1.4 min, while the retention time of PAS was 5.3 min.

**2.12 Ammonia assay**

Unprocessed and spray dried samples were analysed using an ammonia assay kit (Sigma-Aldrich, Ireland) as previously described [7]. Approximately 0.1 mg of the raw material or spray dried samples was accurately weighed and dissolved in 10 ml of water. 1.0 ml of ammonia assay reagent (KGA and NADPH) was accurately transferred into appropriately marked cuvettes. The limit of detection of the assay method used was determined to be 1 µg/ml of ammonia.

**2.13 Scanning Electron Microscopy (SEM)**

Scanning electron micrographs of powder samples were taken using a Hitachi S-4300N instrument (Hitachi Scientific Instruments Ltd., Japan) variable pressure scanning electron microscope. The dry powder samples were fixed on an aluminium stub with double-sided adhesive tabs and a 10-nm-thick gold film was sputter coated on the samples before visualisation [9]. The images were formed from the collection of secondary electrons.

**2.14 Particle Size Analysis**

The particle size distribution was determined by laser diffraction using a Malvern Mastersizer 2000 (Malvern Instruments Ltd., Worcestershire, UK) with the Scirocco 2000 accessory. The dispersive air pressure employed was 2 bar [7]. Samples were run at a vibration feed rate of 60% to obtain obscuration values between 0.5-6% and setting the refractive and absorption indices to 1.4 and 0.01, respectively. The particle size of each sample was determined in triplicate.

**2.15 Density Measurements**

Bulk density (*bp*) was measured as previously described [6] by filling dry powders in a 1 ml graduated syringe (Lennox Laboratory supplies, Ireland) with a funnel. The weight of the powder required to fill 1 ml graduated syringe was recorded in order to calculate *bp*. The tap density (*tp*) of the powder was then evaluated by manually tapping the syringe onto a level surface until constant volume. The resultant volume was recorded in order to calculate *tp*. The tapped density was calculated as the ratio of the mass to the tapped volume of the sample.

### 2.16 *In vitro* aerosol characterisation

The apparatus used was a twin stage impinger (TSI) conforming to the specification in the British Pharmacopoeia [12] and European Pharmacopoeia [13] and the studies were performed similarly as described earlier [9]. The lower stage of the twin impinger has the aerodynamic cut-off diameter of 6.4 µm [14]. A total of 20 ± 1 mg of powder was loaded into a No. 2 hard gelatin capsule. The powders were aerosolised using a dry powder inhalation device (Spinhaler®). The Spinhaler® was attached to the impinger which contained 7 and 30 ml of collecting solvents (80% ethanol) in stages 1 and 2, respectively. An air flow of 60 l/min for 5 s was applied to the TSI. The liquids in stages 1 and 2 were collected and diluted as appropriate and measured by UV spectrophotometry (Pharmspec UV-1700, Shimadzu) at 280 nm for micronised and spray dried PAS and at 271 nm (due to ionisation of PAS) for other systems. Absorbance values were converted to concentrations using calibration curves covering the range of sample concentrations from 0.002 to 0.01 mg/ml. Each deposition experiment involved the aerosolisation of one capsule. Emitted dose was defined as the total quantity of the drug recovered from the upper and lower stages of the impinger and expressed as percent of the total dose loaded into the capsule. Fine particle fraction (FPF) was calculated as the amount deposited in the lower stage as a percentage of the emitted dose. All systems were analysed in triplicate.

### 2.17 Statistical analysis

Statistical analysis was carried out using Minitab™ statistical software. One-way analysis of variance (ANOVA) followed by Tukey test was carried out at a significance level of 0.05, with a p-value of less than 0.05 indicating that the observed difference between the means was statistically significant.

## 3. Results and discussion

### 3.1 Spray drying of PAS from aqueous-alcoholic solutions.

PAS raw material was crystalline, as shown by SEM (Figure 2a) and pXRD (Figure 3a). Solubility studies were first undertaken to estimate the maximum solubility of PAS in the various ethanol/water systems. An increase in PAS solubility with increasing ethanol content in the mix was observed and the drug solubility ranged from 3.66±0.20% w/v for 70% v/v ethanol through 4.03±0.13% w/v for 80% v/v ethanol to 4.49±0.08% w/v for 90% v/v ethanol. Solutions of PAS (1-4%) were prepared in aqueous-ethanolic solvents (70-90% ethanol) and spray dried using an inlet temperature of 78 °C. The products produced had pXRD patterns similar to the raw material (not shown), but consisting of porous particles as well as small rod shaped crystals of PAS as shown in the SEM micrographs (Figures 2b-d). Thus, in contrast to many APIs, PAS remains crystalline on spray drying. Increasing the ethanol content of the spray liquid in the range 70 to 90% v/v seemed to increase the proportion of spherical particulates as assessed by SEM (Figure 2d). An increase in the PAS concentration in the spray dried solution seemed to impact on surface roughness, as observed by SEM (Figures 2d-f), and spray drying of a 4% w/v solution of PAS from 90% (v/v) ethanol resulted in spherical porous particles, rod shaped crystals and spherical crystal clusters (Figure 2f).

Figure 4a shows a DSC scan of crystalline PAS showing only one endothermic event at ~140 °C, consistent with the melting point of PAS reported elsewhere [15]. In the DSC thermogram of PAS spray dried systems, melting endotherms were detected, peaking at

237 ~141-143 ℃ (Figure 4b). PAS is a thermally labile compound, which melts with
238 decomposition [15].

239 The TGA curve for PAS starting material gave a two-stage mass loss with a discontinuity
240 after about 30% mass loss occurring at between approximately 140 and 150 ℃ (Figure 5a).
241 This considerable mass loss may suggest that PAS degraded to 3-aminophenol (the main
242 degradation product of PAS, Figure 1c) in the second stage of the mass loss, consistent with
243 the molecular weight of the 3-aminophenol being app. 70% that of PAS.

244 TGA registered weight losses were 0.67%, 0.77 and 0.95% over the temperature range of
245 25 to 100 ℃ for PAS starting material, PAS spray-dried from 90% (v/v) ethanol and PAS
246 spray-dried from 70% (v/v) ethanol, respectively. The difference in weight loss over the
247 temperature range of 25 to 100 ℃ between starting material and spray-dried samples could
248 be attributed to residual solvent. The shapes of TGA scans were similar for PAS raw
249 material and spray-dried powders.

250

251 **3.2 Spray drying of PAS/ammonium carbonate systems**

252 Healy et al. [6] had previously shown that porous particles could be produced by spray
253 drying systems where ammonium carbonate acted as the process enhancer. Ammonium
254 carbonate (AC) decomposes into ammonia, carbon dioxide and water at temperatures over
255 59 ºC, and the ammonium carbonate was removed from the spray dried system in the
256 exhaust gases producing essentially pure drug particles [6].

257 Solutions of PAS/AC were prepared in 90% v/v ethanol and spray dried. AC in the range of
258 20 to 50% (weight of solids) was added to the solution. A solution of PAS:AC 73:27 w/w was
259 used as it represents the PAS:ammonia 1:1 molar ratio. A system of PAS:AC 62:38 w/w
260 represents PAS:AC 1:1 molar ratio. 20% and 50% AC were also used to study the effect of
261 AC at concentrations lower and higher than the 1:1 molar ratio of PAS:AC. For all these
262 systems the total solid concentration in solution was 3% w/v. Solid, apparently crystalline,
263 spherical agglomerates of particles were produced on spray drying of these systems

(Figures 6a-d). The powder produced by spray drying of PAS:AC 80:20 w/w showed uniform, porous spherical microparticles (Figure 6a).

### 3.2.1 Thermal and pXRD analysis

DSC thermograms of the PAS:AC spray dried systems were all very similar and a representative DSC scan, for the PAS:AC 80:20 w/w system, is shown in Figure 4c. The endothermic peak shifted, the peak broadened and became irregular in shape and asymmetric and there were differences in the onset temperatures for the spray dried system compared to PAS raw material. The onset temperature was ~140˚C with a measured enthalpy of fusion of ~369 J/g for the PAS starting material and 130˚C, with a measured enthalpy of fusion of ~318 J/g for the spray dried sample. It can therefore be concluded that the solid state of the recovered particles was different to unprocessed PAS, suggesting that spray drying of PAS/AC resulted in a new solid state regardless of the amount of AC used in the spray drying process.

Due to the acidic nature of PAS, a chemical reaction between PAS and AC could yield the ammonium salt of PAS (AM-PAS) during processing, with the loss of carbonate as carbon dioxide. Therefore the ammonium salt of PAS was prepared by the method of Forbes et al. [8] and its physicochemical properties were compared to those of the spray dried samples. Figure 4d shows the DSC scan of AM-PAS and demonstrates that the thermal behaviour of the PAS:AC 80:20 w/w spray dried sample is different to that of AM-PAS. The shape of the endothermic peaks was different, and the onset of temperature of the first peak was ~127 ˚C compared to ~130 ˚C for the spray dried sample.

TGA of PAS starting material, PAS:AC 80:20 w/w physical mixture and the equivalent spray dried PAS/AC system revealed that the weight loss between 25˚C and 100˚C was approximately 16.3, 7.6 and 0.7% for the PAS/AC physical mixture, spray dried PAS/AC and PAS starting material, respectively (Figures 5a-c). There was an 11-fold increase in the volatile contents of the spray dried sample in comparison to the unprocessed PAS, while the

weight loss between 25 ˚C and 100 ˚C for the spray dried sample was about half the weight loss shown in the TGA scan of the physical mixture of PAS/AC. As ammonium carbonate decomposes into ammonia, carbon dioxide and water at temperatures over 59 ºC, it is expected that its removal will be complete up to 100 ˚C. The difference between observed and calculated mass loss for the physical mix (approximately 20.6%, corresponding to 20% ammonium carbonate and the mass loss contribution from 80% PAS) could be attributed to an interaction between PAS and AC, consistent with a change of colour of PAS and AC mixture which was observed upon mixing.

The pXRD scan of the PAS:AC 80:20 w/w spray dried sample confirms that the material is crystalline, but differs from the starting material both in intensity and peak positions (Figure 3c). pXRD measurements were also made on the PAS:AC 80:20 w/w physical mixture (Figure 3d) and AM-PAS (Figure 3e) and compared to both unprocessed PAS and the PAS/AC spray dried system. The pXRD scan of the spray dried sample provided further evidence of a difference between the spray dried sample, the starting material and the prepared salt of PAS, as the spray dried sample had different peak positions to those of the physical mixture and AM-PAS. The arrows in the graph show which peaks of the spray dried sample were different from the other systems (or where there was absence of a peak) (Figure 3). pXRD scans of the spray dried samples were also compared to that of 3-aminophenol, the main degradation product of PAS (Figure 3c). Investigation of the scans indicated that the changes in solid state of spray dried sample cannot be attributed to the breakdown product. This was further examined by HPLC analysis, which showed that the degradation products measured for both spray dried and starting PAS material were less than 1% w/w and the observed solid-state changes were not attributable to decomposition of PAS. Comparison of pXRD scans of PAS:AC 80:20 w/w physical mixture and the equivalent spray dried system show that the diffractograms differ, suggesting the formation of a material on spray drying with solid state properties which are different to those of the starting drug, its physical mix with AC and AM-PAS.

### 3.2.2 Chemical structure and stoichiometry estimation

$^{1}$H NMR in solution showed that only peaks corresponding to the hydrogen atoms of the benzene ring were recorded either for the PAS unprocessed material or the PAS:AC 80:20 w/w spray dried sample. In contrast, peaks were found at different ppm in the spectrum of AM-PAS, which is attributed to the difference in electronic environment between the acidic and salt forms. Thus NMR analysis suggests that the spray dried system may contain PAS in its unionised state.

In the solid phase, PAS has an absorption band in the IR spectrum due to $NH_2$ vibrations at 3520 $cm^{-1}$, a further band at 3400 $cm^{-1}$ due to the $NH_2$ and/or OH groups and a strong, characteristic band at 1630 $cm^{-1}$ due to the stretching vibration of C=O [16]. The spectrum of pure PAS presented these characteristic signals at 3496 $cm^{-1}$ for the $NH_2$ vibration, signals at 3388 $cm^{-1}$ for the $NH_2$ and/or OH groups and a band at 1652 $cm^{-1}$ for the C=O group (Figure 7a). Although the FTIR scan of the spray dried PAS:AC 80:20 w/w system showed the same characteristic peaks at the same wavenumbers as the PAS starting material (Figure 7b), there were clear differences between the two materials. The spray dried material had new multiple and sharp bands in the region of 3300-3500 $cm^{-1}$ and broader peaks at 3346 and 3607 $cm^{-1}$ in addition to the two bands at 3388 and 3496 $cm^{-1}$, characteristic of PAS. Some changes were noted in the fingerprint region with two extra absorption bands at 1577 and 1591 $cm^{-1}$ and a region of multiple peaks between 1330 and 1420 $cm^{-1}$. It implies that the chemical structure of PAS in the processed sample remains unchanged, as suggested by HPLC and NMR, the drug molecules remain unionised and new OH and/or NH groups were introduced suggesting that the new material may be a solvated co-crystalline form [10].

In order to determine the stoichiometry of the spray dried PAS/AC, several analyses were undertaken including an ammonia assay for determination of ammonia content, determination of water content by Karl Fischer titration and elemental (CHN) analysis (Table

2). CHN analysis showed that the chemical composition of the spray dried sample differed from that of PAS starting material and of AM-PAS. Elemental analysis also showed that the carbon content of the spray dried sample was lower than the carbon content of the starting material; however, this is higher than the carbon content of AM-PAS. The nitrogen content of the spray dried sample was higher than nitrogen content of the starting material but lower than that of AM-PAS, providing further evidence that the spray dried sample is not the 1:1 ammonium salt.

Ammonia content analysis of unprocessed PAS showed that the amount of ammonia in this sample was below the limit of detection of the assay. The amount of ammonia determined in the PAS/AC 80:20 w/w spray dried sample was 5.2±0.9%, while the amount of water detected was 2.1±0.1%. Therefore the proposed stoichiometry of the PAS/AC spray dried composite is 2:1:0.5 PAS:ammonia:water. Further confirmation of the stoichiometry of spray dried sample was obtained by TGA. TGA revealed that the weight loss between 25℃ and 100℃ was approximately 7.6% for the spray dried composite. The loss of one ammonia molecule and half water molecule corresponds to a loss of ~7.8% by weight of PAS:ammonia:water 2:1:0.5 when determined on a molecular weight basis. Therefore, the weight loss registered in spray dried composites is consistent with the loss of one molecule of ammonia and half molecule of water.

Spray drying of the PAS/AC solutions at a higher inlet temperatures of 120°C, resulted in DSC and pXRD patterns (not shown) for the spray dried material which were similar to PAS presumably as a result of the removal of the attached ammonia from the “solvated” form. Thus inlet temperature has a profound effect on the solid state composition of the powder produced.

### 3.3 Spray drying of the ammonium salt of PAS

A 3% (w/v) solution of AM-PAS was spray dried from 90% (v/v) ethanol. The DSC thermogram of the spray dried sample showed an endothermic event with an onset

temperature of melting at ~120 ˚C. Another small endothermic peak was visible at approximately ~ 86 ˚C (Figure 4e). TGA of the sample showed a loss of approximately 11% of total solid mass in the same temperature region as this endotherm (Figure 5d). This weight loss is consistent with the loss of ammonia (the loss of one ammonia molecule corresponds to a loss of ~10% by weight for the ammonium salt of PAS). This endothermic peak was absent on the DSC scan of the spray dried sample after heating of the sample to 100 ˚C in the DSC and cooling, which likely reflects evaporation of ammonia.

The pXRD scan for AM-PAS spray dried from 90% ethanol showed a different pattern (Figure 3f) in comparison with the starting material (Figure 3e); peak positions were different and extra peaks were found on examination of the diffractogram of the spray dried sample. Furthermore, this diffractogram was comparable to that of the PAS:AC 80:20 w/w spray dried system (Figure 3c). The results of pXRD analysis suggests that spray drying of AM-PAS yielded a material which was similar in solid state nature to that obtained by co-spray drying PAS and AC. The powder produced by spray drying the ammonium salt is shown to consist of spherical agglomerates of particles (Figure 6e) and thus, this system is morphologically different to that of the PAS:AC 80:20 w/w spray dried system.

The results of pXRD analysis suggest that the salt was at least partially converted to the acidic form upon spray drying. This hypothesis is supported by different studies found in the literature concerning thermal decomposition of ammonium salts and recovery of the parent acid by heating of ammonium salts [17, 18, 19]. Guseinov et al. [17] reported that the ability of ammonium salts to undergo thermal decomposition with the formation of gaseous ammonia and free acid is well known. In addition, thermal decomposition of ammonium salts can proceed both in the solid phase, by the heating of the dry salt in a stream of inert gas [17] and in the liquid phase, by heating the aqueous solution of the salt [18]. Furthermore, Chuck and Zacher [19] reported that an aqueous solution of ammonium nicotinate was converted to nicotinic acid by spray drying a solution of ammonium nicotinate (inlet temperature 170-250 ℃); the authors reported that ammonium nicotinate decomposes

during the spray drying process and ammonia, together with the solvent, escape in the exhaust gas of the spray dryer.

Elemental analysis of the spray dried sample of AM-PAS is shown in Table 2. On comparison of the spray dried sample to that of PAS starting material, it is obvious that this inlet temperature did not result in the complete conversion of the salt to the equivalent acid form. Indeed, the inlet temperatures used by Chuck and Zacher [19] were relatively high (170-250 ℃) compared to the milder conditions in the current work (78 °C). The salt seems to transform to the acid form, but the ammonia and water become bound in the crystal lattice leading to the formation of a mixed ammonia-hydrate, like that formed by co-spray drying PAS and AC. This is further confirmed by FTIR analysis (Figure 7c and d) as the spectrum of the spray dried salt resembles closer that of the PAS:AC 80:20 w/w spray dried system than that of the PAS (Figure 7a) or the unprocessed salt (Figure 7b).

### 3.4 Micromeritic and *in vitro* deposition properties of systems for inhalation

The PAS systems spray dried with or without AC showed a monomodal size distribution whereas spray dried AM-PAS, in addition to the main mode, presented a small peak at larger particle sizes, perhaps of agglomerated particles (Figure 8). Table 3 presents the micromeritic characteristics of the various systems. The smallest median particle size of the volume distribution, d(0.5), was found for PAS spray dried from 70% ethanol (2.41±0.07 µm), while the greatest d(0.5) was determined for the spray dried AM-PAS (3.67±0.004 µm). Similar trends were observed for d(0.1) and d(0.9), however the difference between the latter was seen to be non-significant for micronised and spray dried PAS. Span values of approximately 1.6 were calculated for SD PAS and SD AM-PAS, indicating broader size distributions relative to micronised PAS (Span of 1.14±0.04) and SD PAS/AC 80:20 w/w (Span of 1.06±0.01).

The bulk (*bp*) and tap (*tp*) densities of the PAS systems were also determined (Table 3). For spray dried PAS without ammonium carbonate the *bp* was 0.104±0.002 g/cm$^3$ and the *tp*

was 0.168±0.009 g/cm$^3$ and for the system of PAS spray dried with AC the *bp* was 0.122±0.003 g/cm$^3$ and the *tp* was 0.167±0.008 g/cm$^3$. In contrast, the *bp* and *tp* measured for micronised PAS were significantly larger compared to SD PAS and SD PAS/AC 80:20 w/w. The decrease in the density values for the spray dried systems could be explained by the presence of porous particles. The *bp* and *tp* densities for the spray dried ammonium salt of PAS were slightly lower than those of the acid-based systems (Table 3).

Since low density particles have been shown to have increased aerosolisation efficiency [7, 20], the *in vitro* deposition properties of the powders were investigated by twin impinger analysis. The systems selected for aerolisation tests comprised a wide range of morphological characteristics of powder produced by spray drying of PAS under different spray drying conditions.

The results of twin impinger analysis are presented in Figure 9. The ratios of dose retained in the device to that emitted were calculated. The greatest ratio is for micronised PAS and is 1.51 (67.2 ± 3.3% device/32.8 ± 3.6% emitted) and the lowest is for SD PAS/AC 80:20 and is 0.46 (31.5 ± 6.0% device/68.5 ± 6.0% emitted). Figure 9 also shows the percentage of dose deposited in stage 2 of the twin impinger i.e. the respirable fraction; these are numerically shown in Table 4. The sample with the best average deposition on stage 2 of twin impinger was SD PAS/AC 80:20, however no statistically significant difference in respirable fractions between the systems investigated was determined. This may be due to the very rough surfaces and non-uniform morphology of particles (Figures 2 and 6) resulting in interlocking of microparticles. Consequently, the spray dried particles, despite their low densities, failed to show improved respirable fractions in contrast to previously published studies on NPMPs [6,7].

## 4. Conclusions

Spray drying of PAS, at concentrations of 1, 3 and 4% w/v from different ethanolic solvents, resulted in crystalline particles. The particle morphology of PAS spray-dried systems varied

depending on the systems spray dried. Spray drying of PAS/AC, resulted in crystalline particles. AC concentration employed in the spray drying process is important to the successful production of NPMPs. The solid state of PAS/AC was changed by spray drying from ethanol, resulting in a complex solvated form with a stoichiometry of the spray dried product of 2:1:0.5 PAS: ammonia: water.

The chemical composition of spray dried PAS/AC was dependent on the inlet temperature and higher inlets resulted in particles partially converted to the acidic form upon spray drying. Care should therefore be taken when spray drying acidic compounds with ammonium carbonate, an often used pore former.

Spray drying proved a successful method of producing microspherical particles, which deposited in the lower region of the twin stage impinger, indicating that they were in the respirable range. Spray dried PAS systems show a potential for pulmonary delivery, as indicated by the acceptable emitted doses relative to the micronised PAS.

## Declarations

### Conflict of interest

The Author(s) declare(s) that they have no conflicts of interest to disclose.

### Funding

SG would like to thank the Egyptian Government for support in the form of a government scholarship; LT, OIC and AMH would like to acknowledge support from the Solid State Pharmaceutical Cluster (SSPC), grant no. 07/SRC/B1158 funded by the Science Foundation Ireland (SFI).

### References

1. Smith CV et al. TB drug discovery: addressing issues of persistence and resistance. *Tuberculosis* 2004; 84: 45–55.

2. Pandey R, Khuller GK. Antitubercular inhaled therapy: opportunities, progress and challenges. *J Antimicrob Chemother* 2005; 55: 430–435.

3. Fox W et al. Studies on the treatment of tuberculosis undertaken by the British Medical Research Council tuberculosis units, 1946–1986, with relevant subsequent publications. *Int J Tuberc Lung Dis* 1999; 3: S231–S279.

4. Reynolds JEF et al. Martindale, The Extra Pharmacopoia. London : Royal Pharmaceutical Society, 1996.

5. Tsapis N et al. Direct lung delivery of para-aminosalicylic acid by aerosol particles. *Tuberculosis* 2003; 83: 379-385.

6. Healy AM et al. Characterisation of excipient-free nanoporous microparticles (NPMPs) of bendroflumethiazide. *Eur J Pharm Biopharm* 2008; 69: 1182-1186.

7. Nolan LM et al. Excipient-free nanoporous microparticles of budesonide for pulmonary delivery. *Eur J Pharm Sci* 2009; 37: 593-602.

8. Forbes RT et al. Dissolution kinetics and solubilities of p- aminosalicylic acid and its salts. Int J Pharm 1995; 126: 199-208.

9. Tajber L et al. Spray drying of budesonide, formoterol fumarate and their composites-II. Statistical factorial design and in vitro deposition properties. *Int J Pharm*. 2009; 367: 86-96.

10. Paluch KJ et al. Solid-state characterization of novel active pharmaceutical ingredients: cocrystal of a salbutamol hemiadipate salt with adipic acid (2:1:1) and salbutamol hemisuccinate salt. *J Pharm Sci* 2011; 100: 3268-3283.

11. Jivani SG, Stella VJ. Mechanism of decarboxylation of *p*- aminosalicylic acid. *J Pharm Sci* 1985; 74: 1274-1282.

12. British Pharmacopoeia, Great Britain : The Stationary Office, 2008.

13. European Pharmacopoeia, 5th Edition, 2007.

14. Hallworth GW, Westmoreland DG. The twin impinger - a simple device for assessing the delivery of drugs from metered dose pressurized aerosol inhalers. *J Pharm Pharmacol* 1987; 39: 966–972.

15. Verreck G et al. Hot stage extrusion of p-amino salicylic acid with EC using $CO_2$ as a temporary plasticizer. *Int J Pharm* 2006; 327: 45–50.

16. Hassan MMA et al. Aminosalicylic acid. In Florey K, eds. Analytical profiles of drug substances. New York : Academic Press, 1981; 10: 1-28.

17. Guseinov EM et al. Thermal decomposition of ammonium nicotinate. *Pharm Chem J* 1981; 15: 749-752.

18. Frenkel AV et al. Thermal decomposition of ammonium salts of nicotinic acid and its analogs in the liquid phase. *Pharm Chem J* 1995; 29: 480-484.

19. Chuck RJ, Zacher U. Process for the preparation of nicotinic acid. US Patent 6077957, 2000.

20. Edwards DA et al. Large porous particles for pulmonary drug delivery. *Science* 1997; 276: 1868-1872.

Table 1. Spray drying conditions for PAS systems. Key: PAS = p-aminosalicylic acid, AM-PAS = ammonium salt of PAS, EtOH = ethanol, AC = ammonium carbonate.

| System | Solvent % v/v | Solid Conc (% w/v) | AC Conc (% w/w) | Outlet Temp (℃) |
|---|---|---|---|---|
| PAS | 70% EtOH | 1.0 | - | 48 |
| PAS | 80% EtOH | 1.0 | - | 45 |
| PAS | 90% EtOH | 1.0 | - | 45 |
| PAS | 90% EtOH | 3.0 | - | 55 |
| PAS | 90% EtOH | 4.0 | - | 42 |
| PAS/AC | 90% EtOH | 3.0 | 20% AC | 44 |
| PAS/AC | 90% EtOH | 3.0 | 27% AC | 50 |
| PAS/AC | 90% EtOH | 3.0 | 38% AC | 46 |
| PAS/AC | 90% EtOH | 3.0 | 50% AC | 50 |
| AM-PAS | 90% EtOH | 3.0 | - | 45 |

Table 2. Elemental analysis of different PAS systems. Key: PAS = p-aminosalicylic acid, AC = ammonium carbonate, AM-PAS = ammonium salt of PAS, SD = spray dried, C = carbon, N = nitrogen, H = hydrogen, Calculated = results of calculation and Found = results of analysis.

| System | | Analysis (%) | | |
|---|---|---|---|---|
| | | C | H | N |
| PAS | Calculated | 54.90 | 4.61 | 9.15 |
| | Found | 54.83 | 4.62 | 8.99 |
| AM-PAS | Calculated | 49.41 | 5.92 | 16.46 |
| | Found | 49.76 | 5.88 | 15.94 |
| SD PAS/AC 80:20 w/w | Found | 50.88 | 5.32 | 12.33 |
| SD PAS/AC 73:27 w/w | Found | 50.63 | 5.29 | 12.60 |
| SD PAS/AC 62:38 w/w | Found | 50.59 | 5.33 | 12.83 |
| PAS:ammonia:water 2:1:0.5 molar ratio | Calculated | 51.06 | 4.59 | 12.76 |
| AM-PAS SD at 78˚C | Found | 50.29 | 5.42 | 15.30 |
| AM-PAS SD at 120˚C | Found | 52.37 | 5.05 | 11.06 |

Table 3. Micromeritic parameters of different PAS systems. Key: PAS = p-aminosalicylic acid, SD = spray dried, bp = bulk density, tp = tap density.

| System | d(0.1) (µm) | d(0.5) (µm) | d(0.9) (µm) | Span | *bp* (g/cm$^3$) | *tp* (g/cm$^3$) |
|---|---|---|---|---|---|---|
| micronised PAS | 1.67±0.022 | 2.90±0.026 | 4.98±0.132 | 1.14±0.04 | 0.230±0.024 | 0.313±0.022 |
| SD PAS | 1.14±0.004 | 2.41±0.072 | 5.18±0.275 | 1.67±0.06 | 0.104±0.002 | 0.168±0.009 |
| SD PAS/AC 80:20 w/w | 1.93±0.055 | 3.38±0.078 | 5.43±0.138 | 1.06±0.01 | 0.122±0.003 | 0.167±0.008 |
| SD AM-PAS | 1.79±0.020 | 3.67±0.004 | 7.75±0.254 | 1.62±0.05 | 0.093±0.002 | 0.133±0.008 |

Table 4. Respirable fractions of different PAS spray dried systems.

| System | Respirable fraction (%) |
|---|---|
| Micronised PAS | 14.8±2.50 |
| SD PAS | 19.2±6.92 |
| SD PAS/AC 80:20 w/w | 24.5±2.86 |
| SD AM-PAS | 17.9±5.83 |

Figure 1 Molecular structures of: a) PAS, b) ammonia salt of PAS and c) decarboxylation of PAS to 3-aminophenol.

Figure 2 SEM micrograph of (a) PAS raw material, (b) PAS spray dried as 1% w/v solution from 70% v/v ethanol, (c) PAS spray dried as 1% w/v solution from 80% v/v ethanol, (d) PAS spray dried as 1% w/v solution from 90% v/v ethanol, (e) PAS spray dried as 3% w/v solution from 90% v/v ethanol (f) PAS spray dried as 4% w/v solution from 90% v/v ethanol at an outlet temperature of 78°C. Note different magnifications of the micrographs.

Figure 3 pXRD scans of (a) PAS starting material, (b) PAS spray dried as 3% w/v solution from 90% v/v ethanol, (c) 3-aminophenol, (d) PAS:AC 80:20 w/w spray dried from 90% ethanol, (e) PAS:AC 80:20 w/w physical mixture, (f) ammonium salt of PAS starting material and (g) ammonium salt of PAS spray dried as 3% w/v solution from 90% v/v ethanol. The arrows in the graph show differences between the diffractograms. Please note that the main peak of the ammonium salt of PAS starting material was capped for clarity purposes.

Figure 4 DSC scans of (a) PAS starting (b) PAS spray dried as 3% w/v solution from 90% v/v ethanol, (c) PAS:ammonium carbonate 80:20 w/w spray dried from 90% ethanol, (d) ammonium salt of PAS starting material and (e) ammonium salt of PAS spray dried as 3% w/v solution from 90% v/v ethanol.

Figure 5 TGA curves of (a) PAS starting material, (b) PAS:AC 80:20 w/w physical mixture, (c) PAS:AC 80:20 w/w spray dried from 90% ethanol and (d) ammonium salt of PAS spray dried as 3% w/v solution from 90% v/v ethanol.

Figure 6 SEM micrographs of PAS/ammonium carbonate spray dried as 3% w/v solutions from 90% v/v ethanol, where the ratio between PAS to AC used was (a) 80:20 w/w (b) 73:27 w/w (c) 62:38 w/w, (d) 50:50 w/w and (e) spray dried ammonium salt of PAS. Please note different magnifications of the micrographs.

Figure 7 FTIR spectra of (a) PAS starting material, (b) PAS:AC 80:20 w/w spray dried from 90% ethanol, (c) ammonium salt of PAS starting material and (e) ammonium salt of PAS spray dried as 3% w/v solution from 90% v/v ethanol.

Figure 8 Particle size distribution of micronised PAS (solid line), SD PAS (dash line), SD PAS:AC 80:20 w/w (dotted line) and SD AM-PAS (dash-dotted line).

Figure 9 Twin impinger analysis of the micronised and spray dried PAS samples. White bars – micronised PAS, hatched bars – SD PAS, crossed bars – SD PAS:AC 80:20 w/w and grey bars – SD AM-PAS.

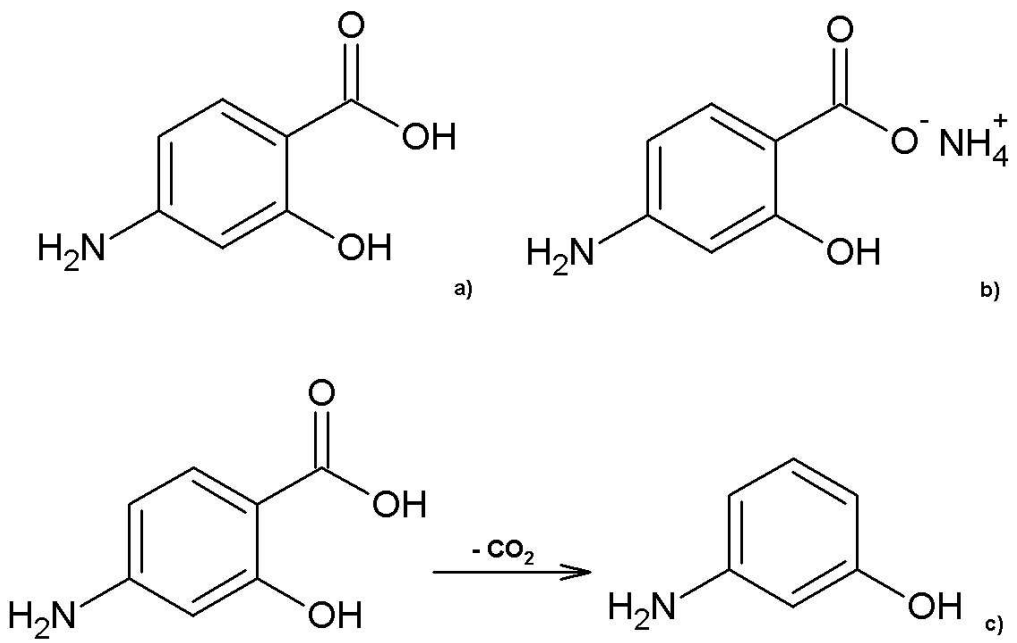


Figure 1 Molecular structures of: a) PAS, b) ammonia salt of PAS and c) decarboxylation of PAS to 3-aminophenol.
296x189mm (96 x 96 DPI)

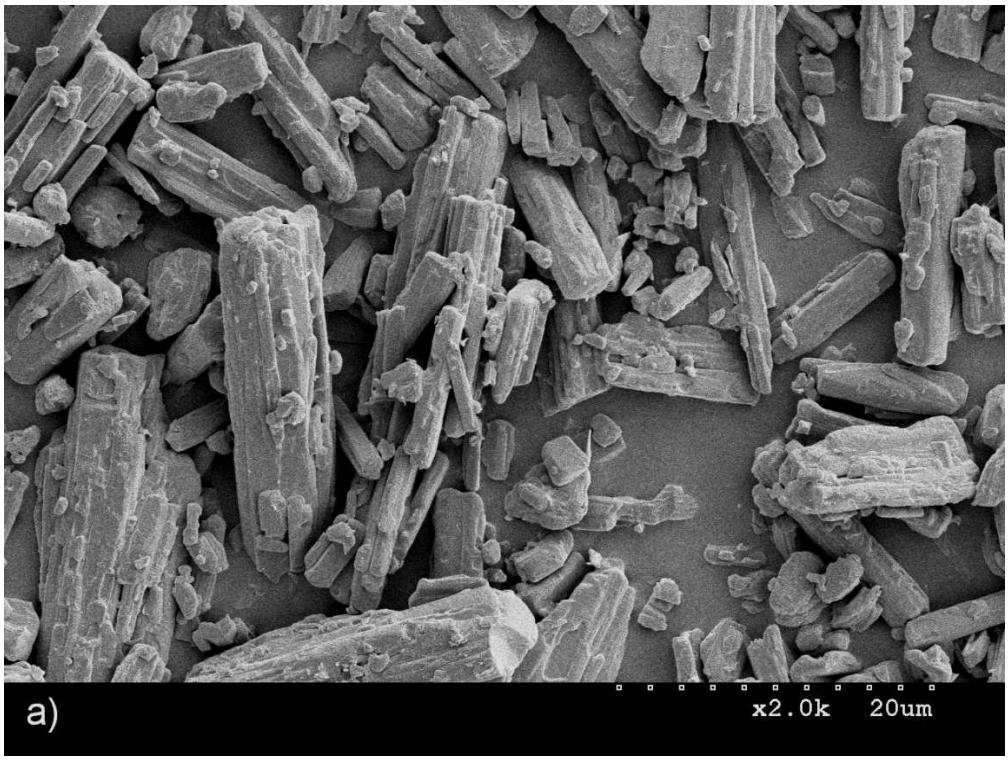


Figure 2 SEM micrograph of (a) PAS raw material, (b) PAS spray dried as 1% w/v solution from 70% v/v ethanol, (c) PAS spray dried as 1% w/v solution from 80% v/v ethanol, (d) PAS spray dried as 1% w/v solution from 90% v/v ethanol, (e) PAS spray dried as 3% w/v solution from 90% v/v ethanol (f) PAS spray dried as 4% w/v solution from 90% v/v ethanol at an outlet temperature of 78 °C. Note different magnifications of the micrographs.
304x228mm (96 x 96 DPI)


304x228mm (96 x 96 DPI)


304x228mm (96 x 96 DPI)

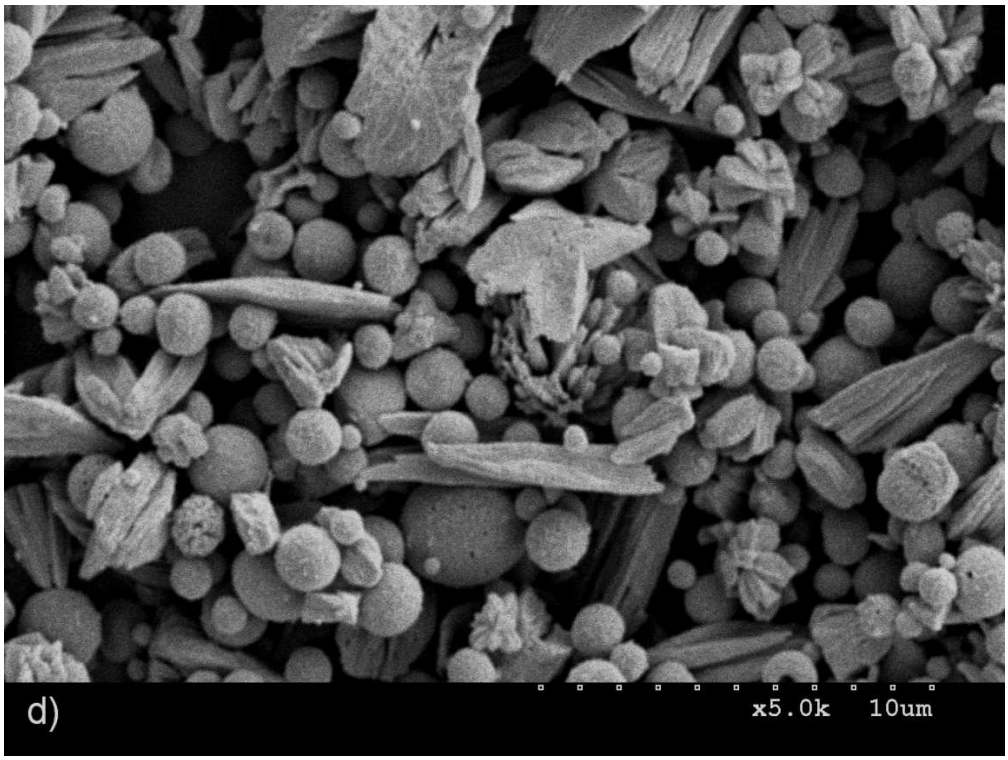


304x228mm (96 x 96 DPI)

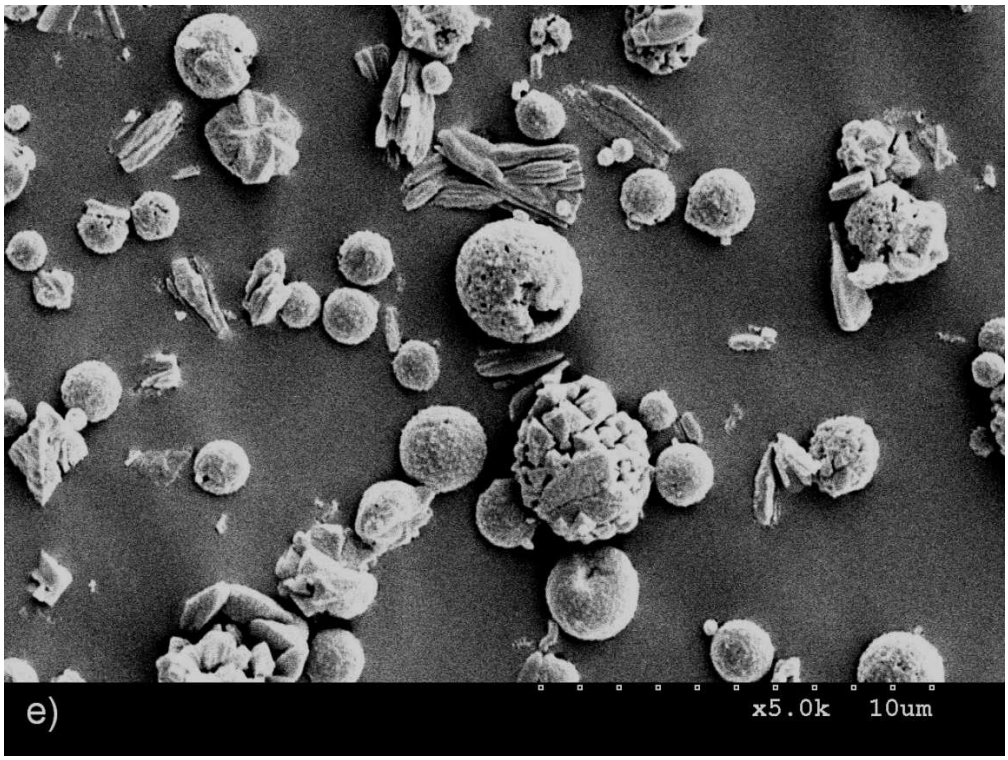


304x228mm (96 x 96 DPI)

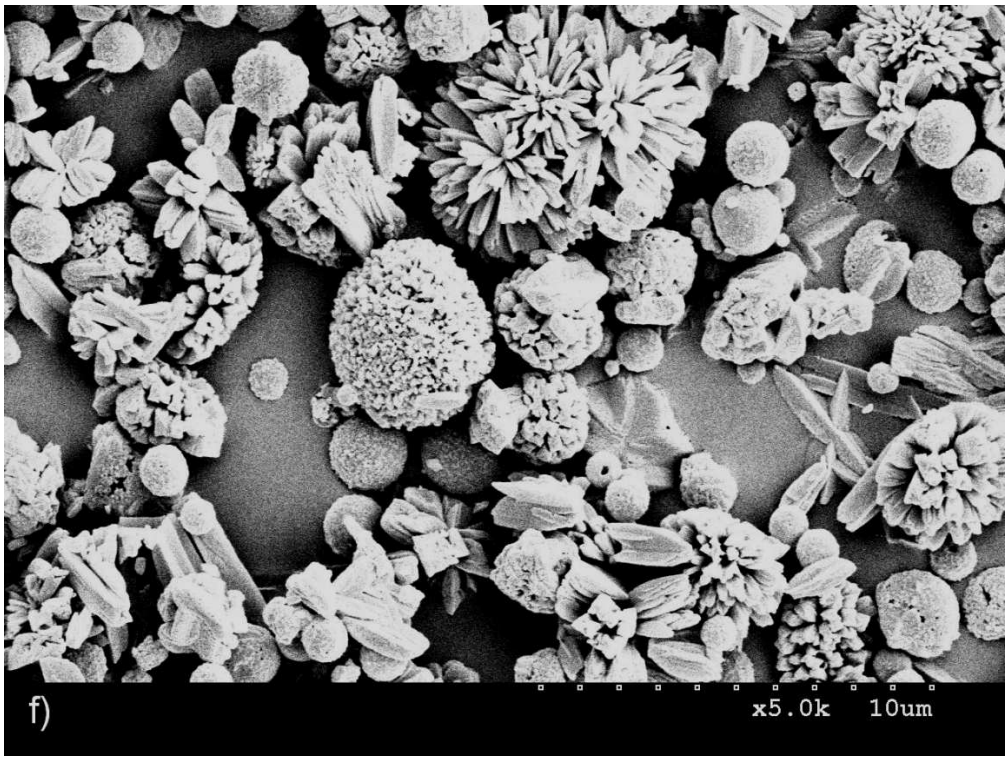


304x228mm (96 x 96 DPI)

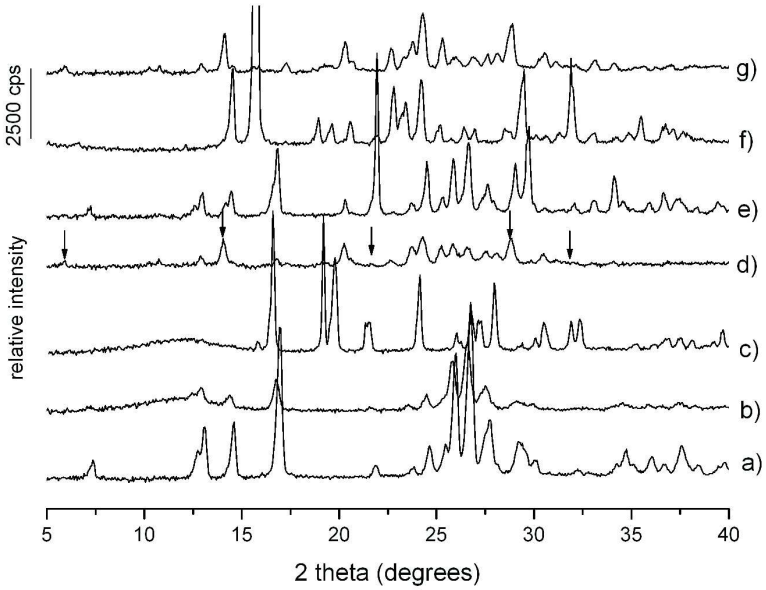


Figure 3 pXRD scans of (a) PAS starting material, (b) PAS spray dried as 3% w/v solution from 90% v/v ethanol, (c) 3-aminophenol, (d) PAS:AC 80:20 w/w spray dried from 90% ethanol, (e) PAS:AC 80:20 w/w physical mixture, (f) ammonium salt of PAS starting material and (g) ammonium salt of PAS spray dried as 3% w/v solution from 90% v/v ethanol. The arrows in the graph show differences between the diffractograms. Please note that the main peak of the ammonium salt of PAS starting material was capped for clarity purposes.
291x203mm (300 x 300 DPI)

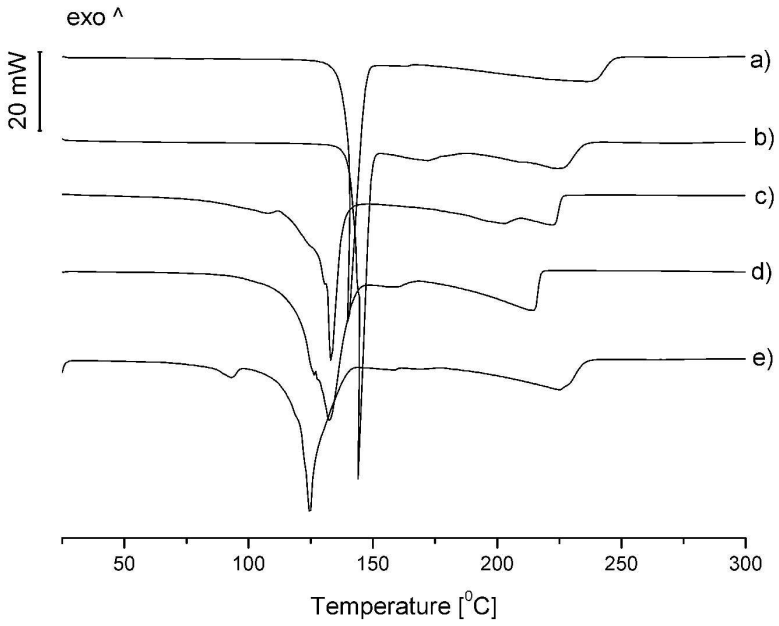


Figure 4 DSC scans of (a) PAS starting (b) PAS spray dried as 3% w/v solution from 90% v/v ethanol, (c) PAS:ammonium carbonate 80:20 w/w spray dried from 90% ethanol, (d) ammonium salt of PAS starting material and (e) ammonium salt of PAS spray dried as 3% w/v solution from 90% v/v ethanol.
291x203mm (300 x 300 DPI)

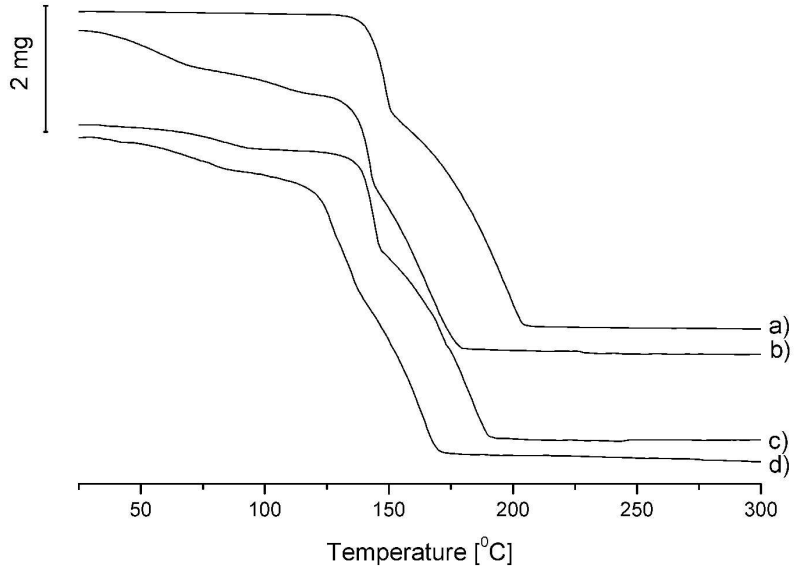


Figure 5 TGA curves of (a) PAS starting material, (b) PAS:AC 80:20 w/w physical mixture, (c) PAS:AC 80:20 w/w spray dried from 90% ethanol and (d) ammonium salt of PAS spray dried as 3% w/v solution from 90% v/v ethanol.
291x203mm (300 x 300 DPI)

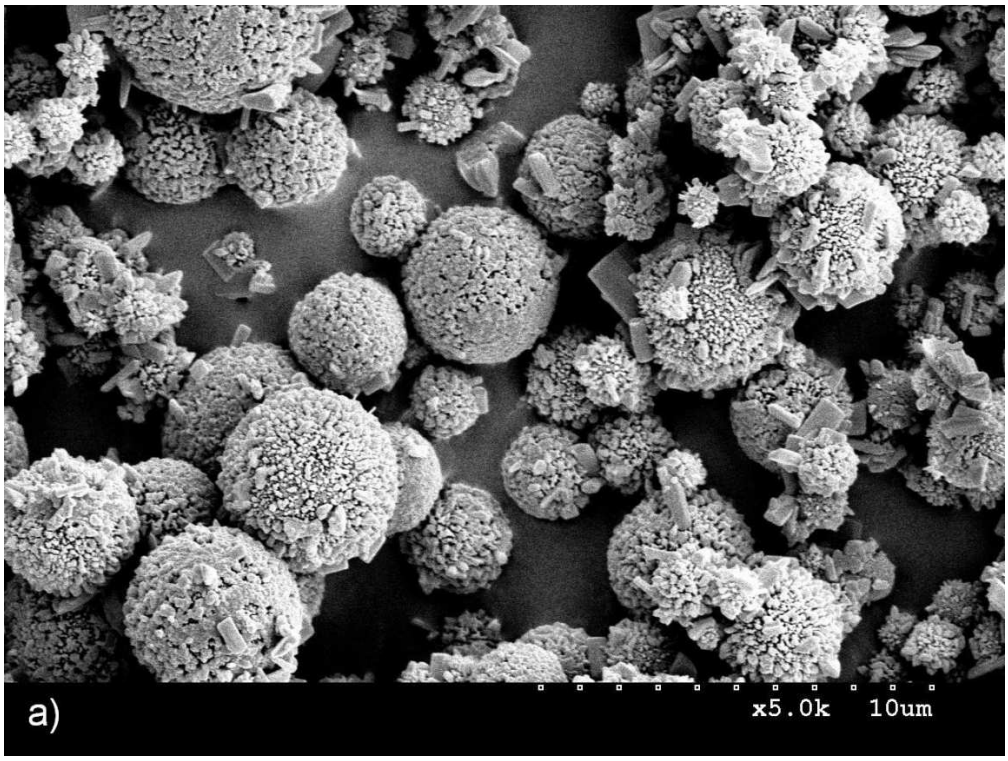


Figure 6 SEM micrographs of PAS/ammonium carbonate spray dried as 3% w/v solutions from 90% v/v ethanol, where the ratio between PAS to AC used was (a) 80:20 w/w (b) 73:27 w/w (c) 62:38 w/w, (d) 50:50 w/w and (e) spray dried ammonium salt of PAS. Please note different magnifications of the micrographs.
304x228mm (96 x 96 DPI)

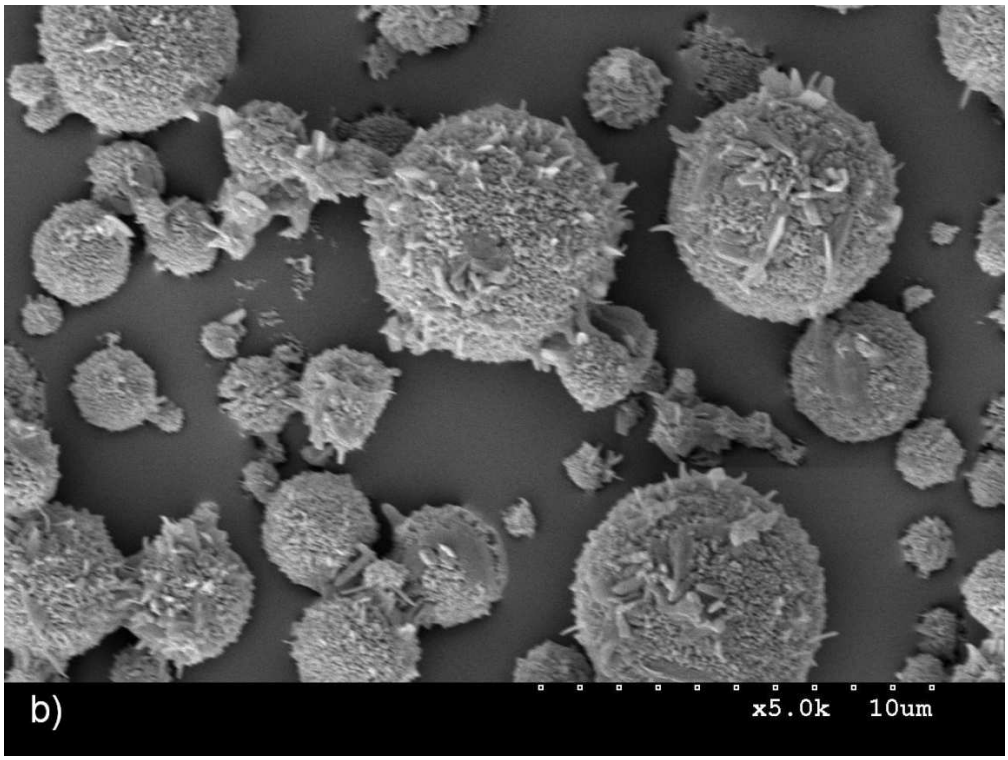


304x228mm (96 x 96 DPI)

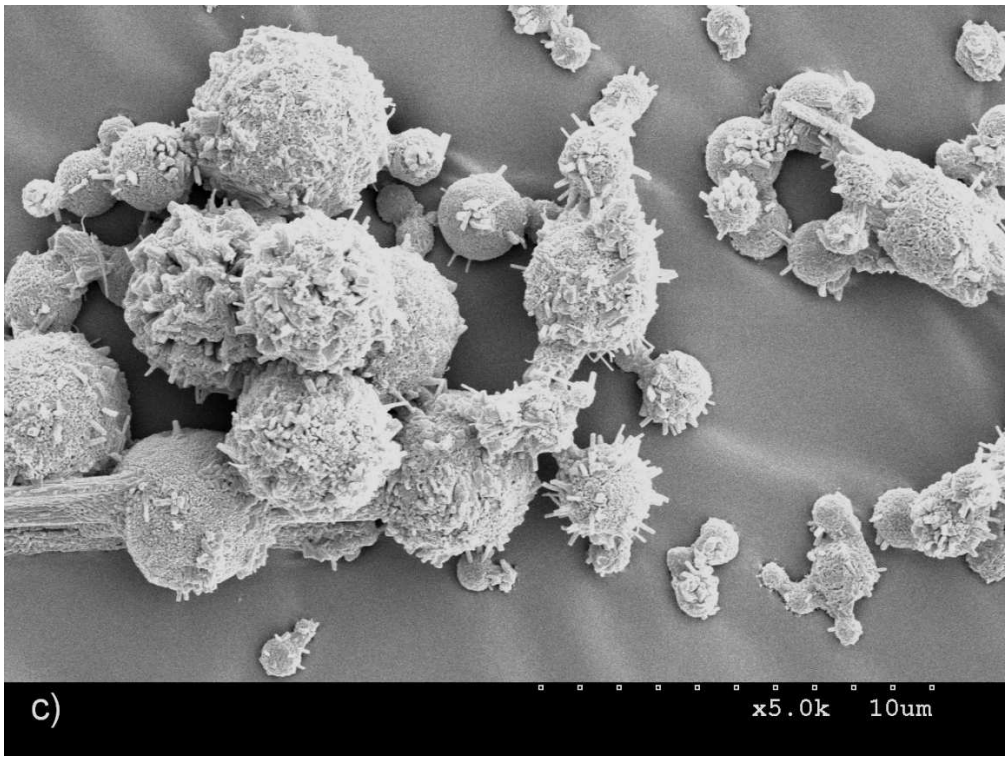


304x228mm (96 x 96 DPI)

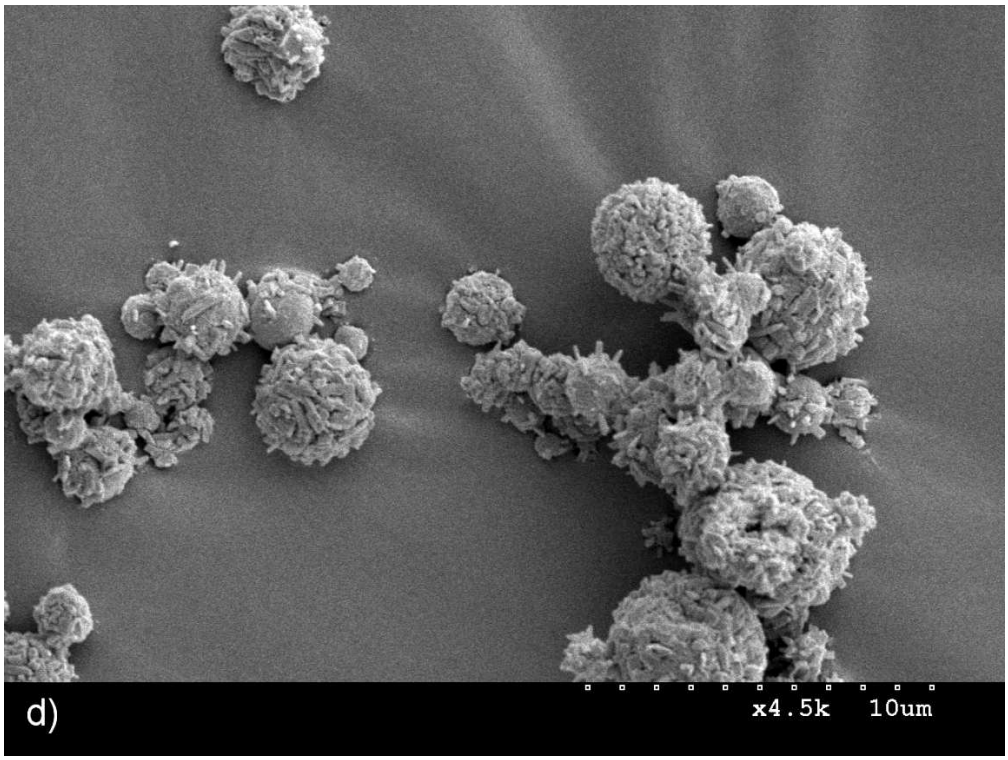


304x228mm (96 x 96 DPI)

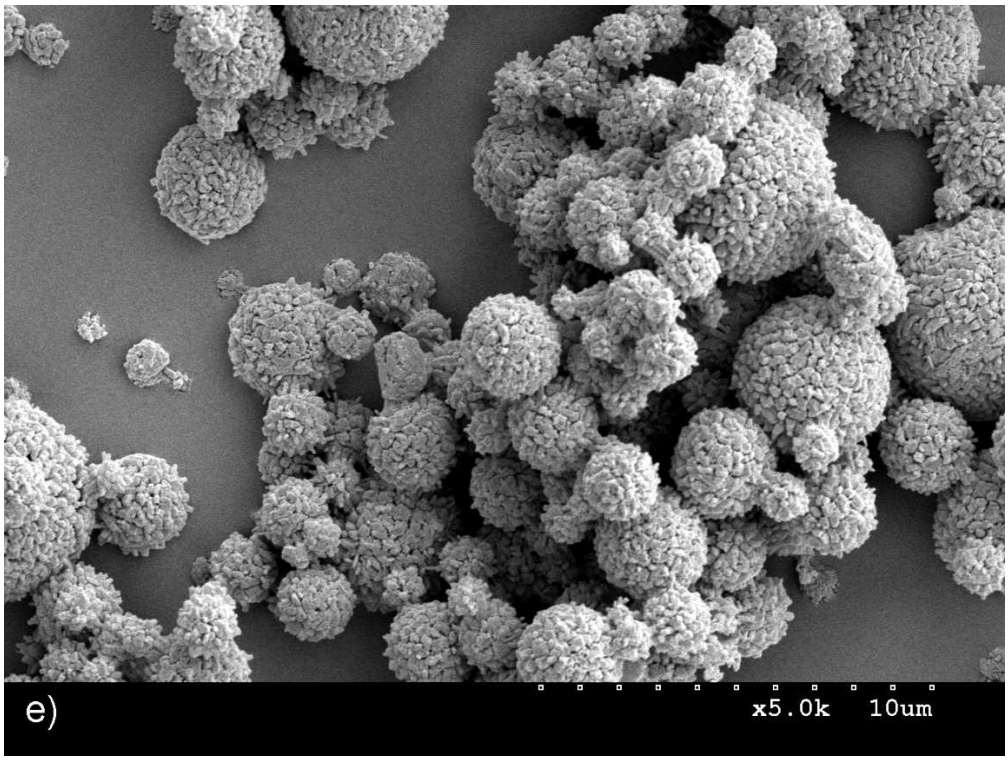


304x228mm (96 x 96 DPI)

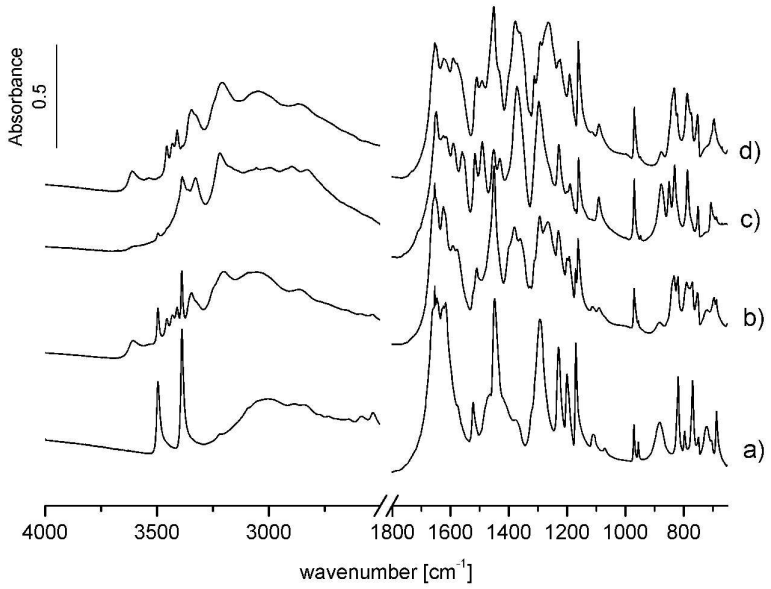


Figure 7 FTIR spectra of (a) PAS starting material, (b) PAS:AC 80:20 w/w spray dried from 90% ethanol, (c) ammonium salt of PAS starting material and (e) ammonium salt of PAS spray dried as 3% w/v solution from 90% v/v ethanol.
281x203mm (300 x 300 DPI)

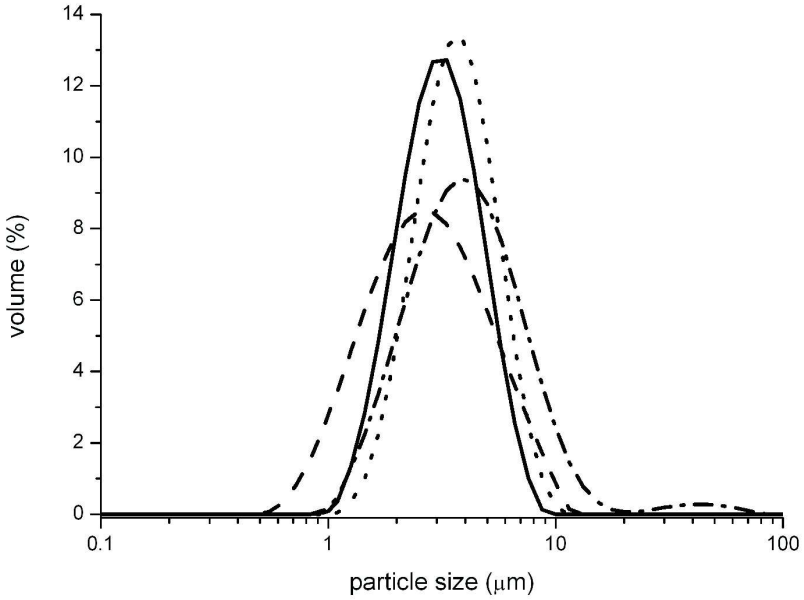


Figure 8 Particle size distribution of micronised PAS (solid line), SD PAS (dash line), SD PAS:AC 80:20 w/w (dotted line) and SD AM-PAS (dash-dotted line).
291x203mm (300 x 300 DPI)

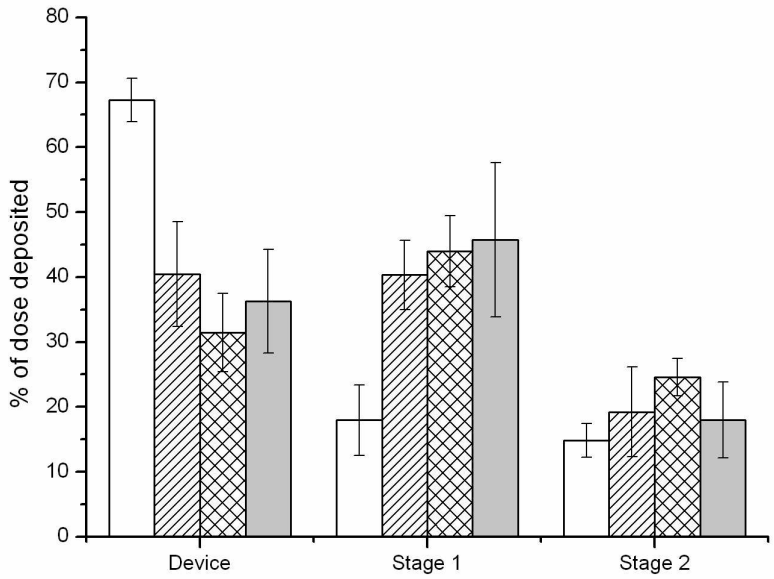


Figure 9 Twin impinger analysis of the micronised and spray dried PAS samples. White bars – micronised PAS, hatched bars – SD PAS, crossed bars – SD PAS:AC 80:20 w/w and grey bars – SD AM-PAS.
281x203mm (150 x 150 DPI)